Effect of Internal Electric Fields on Charge Carrier Dynamics in a Ferroelectric Material for Solar Energy Conversion

Madeleine R. Morris, Stephanie R. Pendlebury, Jongin Hong, Steve Dunn, and James R. Durrant**

There is currently extensive interest in the development of new materials for solar energy utilization, with applications including photovoltaics, artificial photosynthesis, and photocatalysis.[1–3] A key challenge for such solar energy conversion strategies is the minimization of charge recombination losses following light absorption, typically by the use of heterojunctions, redox cascades or electric fields to drive the spatial separation of photogenerated charge carriers.[2,4] One strategy gaining interest to address this challenge is the use of piezoelectric and ferroelectric materials, due to the potential for the internal electric fields present in such materials to aid the spatial separation of charge carriers.[5,6] Enhancements in device efficiency attributed to piezoelectric or ferroelectric effects have been reported for a broad range of photovoltaic, photoelectrochemical, and photocatalytic devices.[7–9] The organohalide lead perovskite materials currently yielding very promising photovoltaic device efficiencies are also reported to be ferroelectric, although the importance of their ferroelectric properties in achieving such high efficiencies is currently unclear.[10–13] In almost all cases where enhanced solar conversion performance has been attributed to ferroelectric materials properties, this enhancement has been assigned to reduced recombination losses.[11,14,15] However to date, to the best of our knowledge, there are no reports directly probing the extent to which spontaneous polarization can indeed increase charge carrier lifetimes. Here, we address this issue, employing transient absorption spectroscopy (TAS) to directly probe the correlation between ferroelectric behavior and carrier lifetimes in a well-established ferroelectric material, $BaTiO_3$.

Ferroelectric materials exhibit a permanent spontaneous polarization (P_s) below a critical temperature known as the Curie temperature (T_C). In this temperature range the unit cell is not centrosymmetric. This leads to the generation of two or more discrete stable polarization states which generate electric fields, known as a spontaneous polarization or dipole.[16] The resultant surface polarization causes band bending (upward where the polarization vector is negative, downward where the polarization is positive), and associated space charge regions. This ferroelectric band bending can exhibit magnitudes of several hundred meV or greater,[17] of similar scale to the band bending present at most p/n and semiconductor/electrolyte junctions employed for solar energy conversion. Indeed, a photovoltage exceeding 16 V has been reported in a photovoltaic device employing $BiFeO_3$, attributed to additive band bending contributions from multiple ferroelectric domains.[18] Band bending associated with the spontaneous polarization of a ferroelectric material, therefore, has the potential to substantially impact on the charge carrier lifetimes, and thus the efficiency, of solar energy conversion devices.

Band bending resulting from the spontaneous polarization of a ferroelectric material has been shown to have significant influence on surface photochemistry. Ferroelectric domain-specific redox reactions have been reported to occur on the surfaces of $BaTiO_3$, $Pb(Zr,Ti)O_3$, and $LiNbO_3$ substrates,[19–21] indicating that the dipole drives electrons and holes to opposite surfaces determined by the direction of the spontaneous polarization and resultant band bending. Recent studies comparing the photocatalytic reactivity of $BaTiO_3$ have shown that tetragonal, ferroelectric $BaTiO_3$ nanoparticles exhibit significantly higher activities than those observed when the dominant crystal phase is the non-ferroelectric cubic phase.[9,22]

Herein we report an investigation, using TAS, of charge carrier dynamics in a prototypical ferroelectric material: $BaTiO_3$. The potential to modulate spontaneous polarization within $BaTiO_3$ through selection of both crystal structure[23] and temperature[24] makes this material an ideal model system to study the impact of the internal fields upon charge carrier dynamics. In particular, we test the hypothesis that the presence of spontaneous polarization-induced band bending can indeed result in increased charge carrier lifetimes. We focus on the charge carrier dynamics on longer (μs–s) timescales as these correspond to carrier lifetimes necessary to drive most photocatalytic or artificial photosynthetic processes, such as water splitting.[25] We find that the tetragonal phase of $BaTiO_3$ exhibits remarkably slow charge carrier recombination ($t_{50\%}$ = 0.12 s). Such

M. R. Morris, Dr. S. R. Pendlebury, Prof. J. R. Durrant
Centre for Plastic Electronics
Department of Chemistry
Imperial College London
London SW7 2AZ, UK
E-mail: j.durrant@imperial.ac.uk
Prof. J. Hong
Department of Chemistry
Chung-Ang University
Seoul 06974, Republic of Korea
Prof. S. Dunn
Materials Research Institute
School of Engineering and Materials
Queen Mary University of London
London E1 4NS, UK
E-mail: s.c.dunn@qmul.ac.uk

DOI: 10.1002/adma.201601238

long carrier lifetimes have not been reported previously for a metal oxide in the absence of chemical scavengers or applied electrical bias. Our results provide direct evidence that the dipoles present in tetragonal $BaTiO_3$ suppress electron/hole recombination. Additionally, we monitor the temperature dependence of charge carrier dynamics in $BaTiO_3$ above and below T_C, and compare ferroelectric and non-ferroelectric phases of $BaTiO_3$ to quantify the influence of the internal dipole on charge carrier recombination.

To investigate the effects of spontaneous polarization on charge carrier dynamics, we conducted experiments on $BaTiO_3$ in both ferro- and non-ferro-electric forms. Single crystal $BaTiO_3$, SC-$BaTiO_3$ (MTI Corporation, (100)-oriented, polarization along *c*-axis), is tetragonal (ferroelectric) at room temperature and cubic (non-ferroelectric) above approximately 120 °C. Thick (≈4 µm) films of $BaTiO_3$ (50 nm diameter nanoparticles), TF-$BaTiO_3$, were deposited on fluorine-doped tin oxide (FTO) conducting glass by screen-printing of $BaTiO_3$ paste (ncsmb000088, NCS Bank, see the Supporting Information for full details). The suppression of ferroelectric behavior in $BaTiO_3$ nanoparticles is well documented in the literature.[9,26–29] The TF-$BaTiO_3$ films studied herein are in the cubic phase and are therefore non-ferroelectric at room temperature (see X-ray diffraction data in Figure S1 in the Supporting Information). Transient absorption measurements were obtained on the µs–s timescale using band-gap excitation at 355 nm (≈150 µJ cm^{-2}, 0.33 Hz, Ar atmosphere), a wavelength at which both samples exhibited strong light absorption (we estimate that the absorption depth will be shorter than the width of the surface band bending, see Figure S2 in the Supporting Information), and probed in the range 460–950 nm.

TAS was employed to monitor excited state absorption in single crystal and thick film $BaTiO_3$. By measuring the change in absorption as a function of both wavelength and time after excitation, information about photoinduced processes such as electron/hole recombination and trapping–detrapping mechanisms can be obtained. The TA spectrum of $BaTiO_3$ under Ar atmosphere is characterized by a broad, featureless positive absorption in the visible range (see Figure S3 in the Supporting Information). Signal intensity generally decreased with increasing probe length. This spectrum is assigned to long-lived photogenerated charge carriers. Such TA signals have been assigned to electron/hole photoinduced absorption in other metal oxides.[30–32]

TA decays of ferroelectric SC-$BaTiO_3$ (see Figure S4 in the Supporting Information for room temperature polarization-electric field loops) and non-ferroelectric TF-$BaTiO_3$ samples are compared in **Figure 1**. Strikingly, at room temperature the tetragonal crystal exhibits a large and long lived transient absorption signal, with a $t_{50\%}$ value (the time taken for the trace to reduce to half of the initial amplitude) of ≈0.12 s. In contrast, the cubic film exhibits a smaller and much shorter lived transient absorption signal, with a decay time at least three orders of magnitude shorter than that of the tetragonal SC-$BaTiO_3$ ($t_{50\%}$ < 100 µs). The fast decay dynamics observed for the TF-$BaTiO_3$ are typical of those observed for non-ferroelectric metal oxides, and assigned to rapid bulk recombination losses.[25,31,33] Such rapid recombination losses have been reported for numerous non-ferroelectric metal oxides with a range of crystal phases, crystallinities, and morphologies. In contrast, lifetimes on the seconds timescale comparable to the SC-$BaTiO_3$ have only

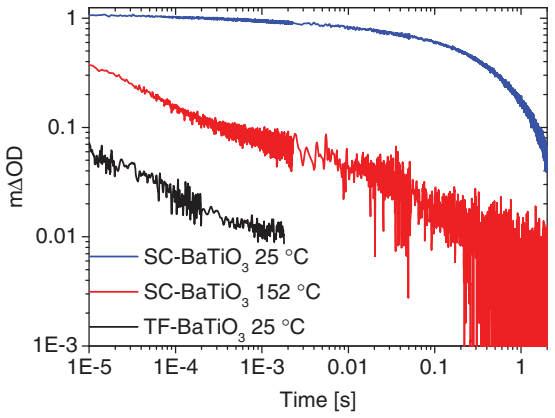

Figure 1. Transient absorption decays (355 nm, ≈150 µJ cm^{-2} excitation; probed at 550 nm under an argon atmosphere) of ferroelectric single crystal $BaTiO_3$ (SC-$BaTiO_3$) at 25 and 152 °C, and non-ferroelectric thick film $BaTiO_3$ (TF-$BaTiO_3$) at 25 °C. At room temperature, SC-$BaTiO_3$ exhibits very long lived charges, but at 152 °C exhibits decay kinetics comparable to those of TF-$BaTiO_3$, consistent with a loss of ferroelectricity above the Curie temperature.

previously reported in metal oxide systems in the presence of strong electrical bias or sacrificial reagents to suppress recombination of photogenerated electrons and holes. The observation of a 0.12 s decay time for SC-$BaTiO_3$ in the absence of any sacrificial species or applied electrical bias is remarkable, and strongly indicative of a process or field in this material driving a very effective spatial separation of charge carriers.

In order to further investigate the origin of the markedly long carrier lifetimes observed in our SC-$BaTiO_3$ sample, we repeated our transient absorption studies upon this sample heated to 152 °C, as shown in Figure 1, red trace. This temperature is above $BaTiO_3$'s Curie temperature T_C, causing the material to undergo a phase transition to the non-ferroelectric cubic phase.[34] It is apparent that this heat treatment results in a pronounced acceleration of the charge carrier decay dynamics. Indeed, the 152 °C SC-$BaTiO_3$ decay dynamics are equivalent, apart from being larger in amplitude, to those of the room temperature non-ferroelectric TF-$BaTiO_3$. This result confirms that the longer carrier lifetimes observed at room temperature for SC-$BaTiO_3$ do not result from the single crystal form of this sample. Rather our data strongly suggest that the ferroelectric properties of the tetragonal $BaTiO_3$ dipole are responsible for the long-lived transient absorption signals observed below T_C for our SC-$BaTiO_3$ sample. They indicate a "switching off" of the internal electric field above T_C which results in a faster recombination rate that is similar to the cubic phase at room temperature. The change in recombination dynamics between room temperature and 152 °C was observed to be reversible, consistent with the previously reported reversible switching of $BaTiO_3$ between tetragonal ferroelectric and cubic non-ferroelectric phases above and below T_C.[35]

We now turn to a more quantitative analysis of the charge carrier lifetimes in SC-$BaTiO_3$ as a function of temperature and therefore ferroelectric polarization. Variable-temperature (25 to 152 °C) transient absorption decays of SC-$BaTiO_3$ using excitation and probe wavelengths of 355 and 550 nm, respectively, are shown in **Figure 2**. It is apparent that the decays are biphasic. They can be fitted to a sum of a stretched exponential

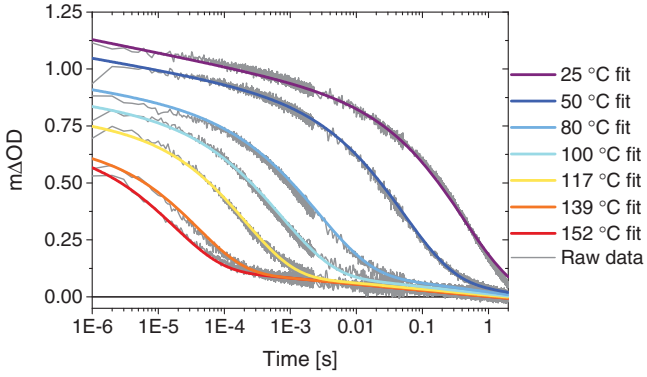

Figure 2. Biphasic transient absorption decays of SC-$BaTiO_3$ as a function of temperature, excited using 355 nm laser light (150 μJ cm^{-2}, 0.33 Hz) and probed at 550 nm, measured from 25 to 152 °C under Ar atmosphere. Raw data are shown in gray for each temperature. Overlaid are the fitted data (a combination of stretched exponential and logarithmic decay phases).

(where $\beta = 1$ corresponds to a monoexponential decay) and logarithmic decays according to the equation:

$$\Delta OD(t) = Ae^{-\left(\frac{t}{\tau}\right)^{\beta}} + B\log_{10}\left(\frac{C}{t}\right) \quad (1)$$

Full details of the fitting parameters as a function of temperature are included in the Supporting Information. The stretched exponential component, which dominates the decay dynamics at all temperatures, shows a strong temperature dependence in lifetime, τ, while the stretch exponent, β, remains approximately constant (0.58 ± 0.03) across the temperature range. As the strength of the dipole associated with the ferroelectric nature of the sample decreases with increasing temperature below T_C, the strong temperature dependence of this decay phase suggests it is related to the temperature dependence of the dipolar crystal structure, as we discuss further below.

The second, logarithmic, decay phase appears to be relatively temperature independent, and is most apparent as weak tails in the transient decays in the higher temperature data. This logarithmic decay phase also was observed to be more prominent at longer probe wavelengths (see Figure S5 in the Supporting Information). This phase is tentatively assigned to tunneling recombination from deeply trapped carriers. In any case, its temperature independence indicates that this decay phase is not related to ferroelectricity, and is therefore not considered further herein.

The magnitude of the temperature dependence of the carrier lifetime apparent from Figure 2 is remarkably high, corresponding to a four orders of magnitude acceleration of the dominant, stretched exponential phase for a temperature increase from 298 to 425 K. This temperature dependence can be most conveniently quantified by an Arrhenius type analysis, as illustrated in **Figure 3**. This figure shows that $t_{50\%}$ values of the stretched exponential decay phase in SC-$BaTiO_3$ displays an exponential dependence on temperature ($t_{50\%} \propto e^{-E_A/k_BT}$) with an apparent activation energy E_A of 0.85 eV. For comparison we include analogous temperature dependent data for another, non-ferroelectric metal oxide, α-Fe_2O_3 (hematite), which

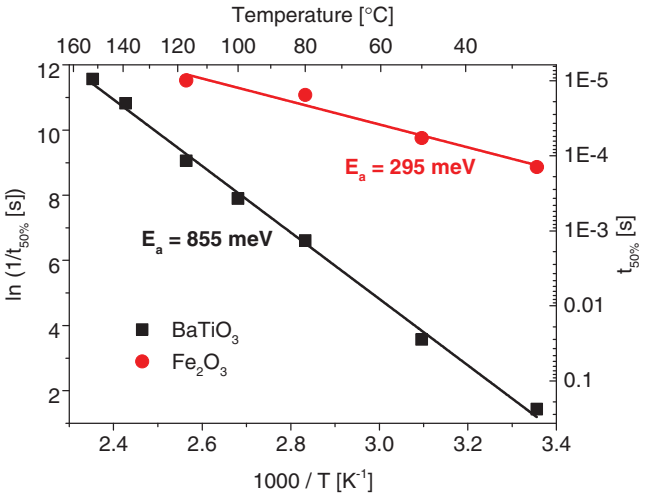

Figure 3. Arrhenius plot showing linear behavior of τ, the faster decay phase (μs–ms) lifetime, with temperature for a single crystal $BaTiO_3$ and a nanostructured α-Fe_2O_3 film. Symbols are experimental data points, the solid lines are the linear fits. An apparent activation energy, E_A, of 855 meV is obtained for $BaTiO_3$ which relates to the band bending within the material. The E_A obtained for Fe_2O_3 is 295 meV.

exhibits much more limited temperature dependence and a correspondingly smaller value for E_A of 0.30 eV. This smaller apparent activation energy is consistent with detrapping-limited charge recombination, with a trap state depth of a few hundred meV, typical for such oxide materials.[25] We attribute the much stronger temperature dependence of the charge carrier lifetime in SC-$BaTiO_3$ to the temperature dependent ferroelectric dipole-induced band bending in this material.

In order to address more quantitatively the origin of the strong temperature dependence of the TA decays shown in Figure 2, we consider further the temperature dependence of the spontaneous polarization (P_S). $BaTiO_3$ has been reported to show a progressive reduction in P_S as the temperature is increased toward T_C, at which point P_S drops to zero.[36] Changes in the crystal structure of a ferroelectric material with temperature are well known and influence the strength of P_S.[37] As $BaTiO_3$ moves from a tetragonal system to a cubic one the non-centrosymmetric nature of the crystal is progressively reduced before making the transition to the fully cubic phase above T_C. Thus, the extent of band bending driven by the depolarization field (and consequently the height of resultant energetic barriers to charge recombination) will decrease with increasing temperature, even for temperatures below T_C. Accepted values for $BaTiO_3$ give P_S reducing approximately linearly from 26 μC cm^{-2} at 30 °C to 20 μC cm^{-2} at 100 °C, a drop of ≈25%.[38,39] Above T_C (≈120 °C for $BaTiO_3$) P_S drops to 0 μC cm^{-2}. Analogous changes in surface potentials have been measured using scanning surface potential microscopy,[24] reporting a reduction in surface potential by 10–20% during heating, before collapsing to approximately zero above T_C. Photoelectron emission spectroscopy studies have indicated a 30% loss of band bending of $BaTiO_3$ during heating in the tetragonal phase below T_C.[40] Such dependencies of P_S and surface potential upon temperature have also been supported by theoretical modeling based on treating the ferroelectric

medium as a polar semiconductor.[41] Regarding the absolute magnitude of the band bending in $BaTiO_3$ resulting from P_S, reported values at room temperature measured under vacuum conditions are of the order of 1.3 V in total or 0.65 V at each interface.[40] We note that band bending is typically reduced under atmospheric conditions, such as those employed herein, by external screening due to molecular chemisorption to the $BaTiO_3$ surface.[42] In our case, the illumination of the surface of the ferroelectric is likely to reduce such screening. It is known that $BaTiO_3$ is a photocatalyst[9] and as such illumination of the sample will cause photocatalytic removal of surface contaminants. Thus the surface band bending for the samples studied herein is likely to lie between that measured for samples under atmospheric conditions and those under vacuum. The previous data available from the literature indicates an approximately linear change of between 10% and 30% of the surface band bending for a $BaTiO_3$ sample over the range ≈30 to ≈100 °C.[24,36,39] Therefore it seems likely that our surface band bending at ≈30 °C will be of the order ≈0.3–0.5 V, reducing by ≈20% upon heating to ≈100 °C. Above T_C it will collapse to ≈0 V as illustrated in **Figure 4**a.

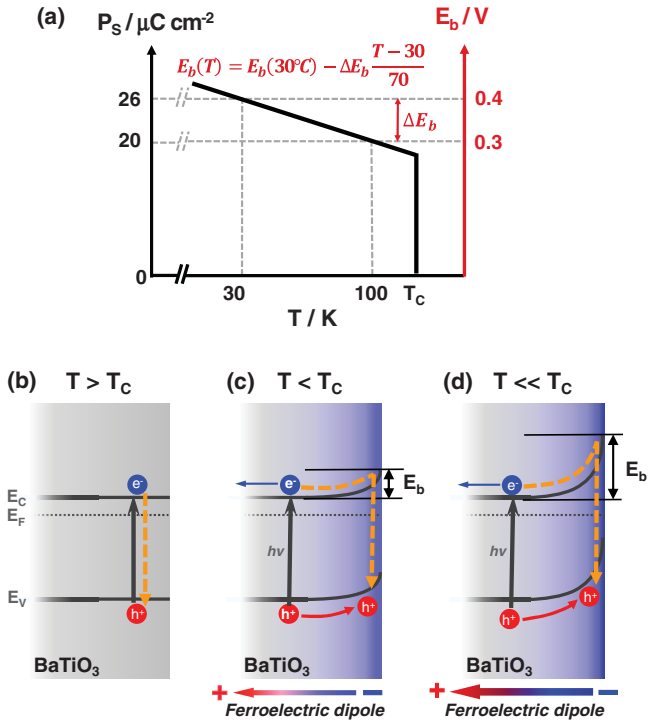

Figure 4. a) Temperature dependence of spontaneous polarization (left axis) and consequent band bending (right axis) in $BaTiO_3$. For this simple model for $E_b(T)$, the relationship has been approximated as a linear correlation below the Curie temperature (T_C) with an abrupt drop to zero at T_C (consistent with a first order phase transition). b–d) Schematic representations of polarization-induced band bending changing with temperature. Above T_C (b) there is no polarization and thus no band bending (for clarity, band bending due to atmospheric effects is omitted here, although it is likely that some upward band bending exists above T_C). Below T_C (c,d), the polarization induces surface band bending which acts as a thermal barrier to electron/hole recombination. Dashed arrows indicate a possible thermally activated recombination pathway of photogenerated electrons in the conduction band (E_C) with photogenerated holes in the valence band (E_V).

We turn now to the likely impact of this temperature dependent band bending on charge carrier recombination. Such band bending can be expected to result in a thermal barrier E_b to charge recombination, as illustrated in Figure 4b, with the recombination time constant therefore expected to show an exponential dependence upon the barrier height. In our case, we assume E_b is decreasing approximately linearly with increasing temperature between 30 and 100 °C such that, $E_b(T) = E_b\ (30\ °C) - \Delta E_b(T-30)/70$ where ΔE_b is the reduction in E_b between 30 and 100 °C. Applying this temperature dependent barrier energy to an Arrhenius type activation energy analysis, we obtain an effective activation energy $E_A^{eff} = E_b(30\ °C) + 4.3\Delta E_b$. In other words, in the presence of a linearly decreasing thermal barrier to charge recombination, we still expect Arrhenius type behavior, but with an increased apparent activation energy E_A^{eff}. Using the values for E_b and ΔE_b obtained from ferroelectric literature (E_b(30 °C) ≈ 0.4 eV and ΔE_b ≈ 0.1 eV), we obtain a value for E_A^{eff} of the order of 0.83 eV, in good agreement with the value of E_A = 0.85 eV measured by our transient absorption data, thus supporting the simple model we employ herein. As such, we conclude that the strong temperature dependence of our observed charge carrier lifetimes in SC-$BaTiO_3$ is in good agreement with the expected temperature dependence of the ferroelectric band bending present in this material.

As further support to this simple model, we note that the magnitudes of the spontaneous polarization-induced band bending used in this model are of similar size to the magnitudes of the electrical bias-induced band bending required in non-ferroelectric photoelectrodes such as Fe_2O_3 to achieve similar carrier lifetimes (0.1–1 s) to those reported herein for $BaTiO_3$.[25] We also note that the absence of a further sharp reduction in carrier lifetime as the temperature is increased above T_C is most probably due to charge trapping effects becoming the dominant limitation on charge carrier recombination on these timescales, as has been reported for other metal oxides.

This study demonstrates that the use of materials with spontaneous polarization-induced band bending, i.e., ferroelectrics, in solar energy systems could significantly increase solar conversion efficiencies in devices which would otherwise be limited by electron/hole recombination. Spontaneous polarization-induced band bending of several hundred meV in the ferroelectric material studied herein is of similar magnitude to the band bending achieved by p/n junctions and semiconductor–electrolyte junctions in solar energy conversion devices, and results in a 10^4 increase in charge carrier lifetimes compared to the non-ferroelectric material. Our studies thus demonstrate that internal fields can indeed result in a spatial separation of charge carriers, and thereby a reduction in charge recombination losses, potentially enhancing solar conversion device performance. For example, the lifetimes observed here match the rate constants of photoelectrochemical water oxidation reported in the literature,[25,43] indicating that ferroelectrics could have a particularly high impact in solar water splitting systems. Further, we have previously shown that even an order of magnitude increase carrier lifetime can result in 100 mV increase in

voltage output of organic solar cells.[44] The magnitude of the effects reported herein also suggest that the presence of ferroelectric domains in organohalide lead perovskites may indeed be sufficient to explain the remarkably long charge carrier lifetimes (corresponding to strongly "non-Langevin" recombination) observed in these materials.[15,45] These long carrier lifetimes have been suggested to be a key factor behind the high efficiencies of perovskite based solar cells.

Our studies furthermore show that optical techniques such as the transient absorption studies employed herein can be used to probe the magnitude of polarization-induced band bending at free ferroelectric surfaces. Despite the extensive body of research on these materials, reports of barrier heights in ferroelectrics associated with this band bending are not well documented in the literature. By employing the simple model described herein, we have shown that it is possible to use variable-temperature transient absorption studies to obtain a band bending value for single crystal $BaTiO_3$ in good agreement with literature-reported values.

In summary, we have shown directly, for the first time, that the internal fields in ferroelectric single crystal $BaTiO_3$ inhibit electron/hole recombination, resulting in long-lived ($t_{50\%}$ = 0.12 s) carriers in the absence of externally applied electrical potential or sacrificial reagents. Switching off the ferroelectric dipole results in rapidly accelerated charge carrier recombination, attributed to a decrease in band bending associated with loss of ferroelectric polarization. By using variable-temperature TAS we have measured an effective activation barrier to electron/hole recombination in single crystal $BaTiO_3$, which relates to the polarization-induced surface band bending. A simple thermodynamic model capable of estimating the magnitude of band bending is proposed. We envisage that this model can be applied to other ferroelectric materials. This study clearly demonstrates the potential for ferroelectrics to significantly increase the efficiency of both solar photovoltaic and solar fuels devices.

Experimental Section

Full experimental details are given in the Supporting Information. Briefly, a $BaTiO_3$ single crystal of dimensions 10 mm × 10 mm × 1 mm and crystallographic orientation (100) (± 0.5°) was studied as received (MTI Corporation, BTOa101010S2), along with $BaTiO_3$ thick (≈4 μm) films (ncsmb00084, Noncentrosymmetric Materials Bank (NCS Bank) prepared by screen printing of a paste of cubic-phase nanoparticles (≈50 nm diameter, ncsmb000080, NCS Bank) onto FTO conducting glass (TEC 8, Pilkington). Transient absorption measurements were obtained using bandgap excitation at 355 nm (0.33 Hz, ≈150 μJ cm^{-2}) and monochromatic probe beam at 550 nm, as described in detail in the Supporting Information and elsewhere.[32]

Supporting Information

Supporting Information is available from the Wiley Online Library or from the author.

Acknowledgements

The authors are grateful to the EPSRC Plastic Electronics CDT (EP/L016702/1), the ERC project Intersolar (291482), and Climate-KIC (GA 2015) for funding, Simon Turner and Steve Atkins for variable-temperature TAS equipment. J.H. acknowledges a Korea-ERC researcher exchange program (NRF-2014K2A7A1044503) and a grant (NRF-2013M2A8A1035822) through the National Research Foundation (NRF) funded by the Ministry of Science, ICT & Future Planning (MSIP) of Korea.

Received: March 3, 2016
Revised: April 12, 2016
Published online: June 9, 2016

[1] L. M. Peter, *Philos. Trans. R. Soc. London, Ser. A* **2011**, *369*, 1840.
[2] Y. Tachibana, L. Vayssieres, J. R. Durrant, *Nat. Photonics* **2012**, *6*, 511.
[3] F. Fresno, R. Portela, S. Suárez, J. M. Coronado, *J. Mater. Chem. A* **2014**, *2*, 2863.
[4] G. Lakhwani, A. Rao, R. H. Friend, *Annu. Rev. Phys. Chem.* **2014**, *65*, 557.
[5] J. J. L. Giocondi, G. S. Rohrer, *J. Phys. Chem. B* **2001**, *105*, 2.
[6] M. Stock, S. Dunn, *IEEE Trans. Ultrason. Ferroelectr. Freq. Control* **2011**, *58*, 1988.
[7] S. Shoaee, J. Briscoe, J. R. Durrant, S. Dunn, *Adv. Mater.* **2013**, *26*, 1.
[8] W. Yang, Y. Yu, M. B. Starr, X. Yin, Z. Li, A. Kvit, S. Wang, P. Zhao, X. Wang, *Nano Lett.* **2015**, *15*, 7574.
[9] Y. Cui, J. Briscoe, S. Dunn, *Chem. Mater.* **2013**, *25*, 4215.
[10] Y. Kutes, L. Ye, Y. Zhou, S. Pang, B. D. Huey, N. P. Padture, *J. Phys. Chem. Lett.* **2014**, *5*, 3335.
[11] J. M. Frost, K. T. Butler, F. Brivio, C. H. Hendon, M. van Schilfgaarde, A. Walsh, *Nano Lett.* **2014**, *14*, 2584.
[12] Z. Fan, J. Xiao, K. Sun, L. Chen, Y. Hu, J. Ouyang, K. P. Ong, K. Zeng, J. Wang, *J. Phys. Chem. Lett.* **2015**, *6*, 1155.
[13] M. Coll, A. A. Gomez, E. Mas-Marza, O. Almora, G. G. Garcia-Belmonte, M. Campoy-Quiles, J. Bisquert, *J. Phys. Chem. C* **2015**, *6*, 1408.
[14] W. Wang, F. Liu, C. Man Lau, L. Wang, G. Yang, D. Zheng, Z. Li, *Appl. Phys. Lett.* **2014**, *104*, 123901.
[15] C. Wehrenfennig, G. E. Eperon, M. B. Johnston, H. J. Snaith, L. M. Herz, *Adv. Mater.* **2014**, *26*, 1584.
[16] B. Jaffe, W. R. Cook, H. Jaffe, W. R. Cooke, *Piezoelectric Ceramics*, Academic Press, London, UK **1971**.
[17] S. Dunn, D. Tiwari, *Appl. Phys. Lett.* **2008**, *93*, 092905.
[18] S. Y. Yang, J. Seidel, S. J. Byrnes, P. Shafer, C.-H. Yang, M. D. Rossell, P. Yu, Y.-H. Chu, J. F. Scott, J. W. Ager, L. W. Martin, R. Ramesh, *Nat. Nanotechnol.* **2010**, *5*, 143.
[19] Y. Inoue, I. Yoshioka, K. Sato, *J. Phys. Chem.* **1984**, *209*, 1148.
[20] J. J. L. Giocondi, G. S. Rohrer, *Chem. Mater.* **2001**, *13*, 241.
[21] S. V Kalinin, D. A. Bonnell, T. Alvarez, X. Lei, Z. Hu, J. H. Ferris, Q. Zhang, S. Dunn, *Nano Lett.* **2002**, *2*, 589.
[22] Y. Cui, S. M. Goldup, S. Dunn, *RSC Adv.* **2015**, *5*, 30372.
[23] H. Search, C. Journals, A. Contact, M. Iopscience, C. L. Wang, S. R. P. Smith, *J. Phys.: Condens. Matter* **1995**, *7*, 7163.
[24] S. V. Kalinin, D. A. Bonnell, *J. Appl. Phys.* **2000**, *87*, 3950.
[25] M. Barroso, S. R. Pendlebury, A. J. Cowan, J. R. Durrant, *Chem. Sci.* **2013**, *4*, 2724.
[26] M. H. Frey, D. A. Payne, *Phys. Rev. B.: Condens. Matter Mater. Phys.* **1996**, *54*, 3158.
[27] B. Begg, E. Vance, J. Nowotny, *J. Am. Ceram. Soc.* **1994**, *77*, 3186.
[28] F. Yen, H. Hsiang, Y. Chang, *Jpn. J. Appl. Phys.* **1995**, *34*, 6149.
[29] K. Uchino, E. Sadanaga, T. Hirose, *J. Am. Ceram. Soc.* **1989**, *72*, 1555.
[30] Y. Ma, S. R. Pendlebury, A. Reynal, F. Le Formal, J. R. Durrant, *Chem. Sci.* **2014**, *5*, 2964.
[31] S. R. Pendlebury, M. Barroso, A. J. Cowan, K. Sivula, J. Tang, M. Grätzel, D. Klug, J. R. Durrant, *Chem. Commun.* **2011**, *47*, 716.

[32] J. Tang, J. R. Durrant, D. R. Klug, *J. Am. Chem. Soc.* **2008**, *130*, 13885.
[33] Z. Huang, Y. Lin, X. Xiang, W. Rodríguez-Córdoba, K. J. McDonald, K. S. Hagen, K.-S. Choi, B. S. Brunschwig, D. G. Musaev, C. L. Hill, D. Wang, T. Lian, *Energy Environ. Sci.* **2012**, *5*, 8923.
[34] Y. Bai, K. Ding, G.-P. Zheng, S.-Q. Shi, L. Qiao, *Phys. Status Solidi* **2012**, *209*, 941.
[35] H. D. Megaw, *Proc. Phys. Soc.* **1946**, *58*, 340.
[36] W. J. Merz, *Phys. Rev.* **1953**, *91*, 513.
[37] H. F. Kay, P. Vousden, *Philos. Mag. J. Sci.* **1949**, *40*, 1019.
[38] W. J. Merz, *Phys. Rev.* **1953**, *91*, 513.
[39] T. Lee, I. A. Aksay, *Cryst. Growth Des.* **2001**, *1*, 401.
[40] A. Höfer, M. Fechner, K. Duncker, M. Hölzer, I. Mertig, W. Widdra, *Phys. Rev. Lett.* **2012**, *108*, 087602.
[41] H. Matsuura, *New J. Phys.* **2000**, *2*, 8.
[42] S. V Kalinin, C. Y. Johnson, D. A. Bonnell, *J. Appl. Phys.* **2002**, *91*, 3816.
[43] A. J. Cowan, C. J. Barnett, S. R. Pendlebury, M. Barroso, K. Sivula, M. Grätzel, J. R. Durrant, D. R. Klug, M. Grätzel, J. R. Durrant, D. R. Klug, *J. Am. Chem. Soc.* **2011**, *133*, 10134.
[44] C. G. Shuttle, B. O'Regan, A. M. Ballantyne, J. Nelson, D. D. C. Bradley, J. R. Durrant, *Phys. Rev. B: Condens. Matter Mater. Phys.* **2008**, *78*, 1.
[45] C. Wehrenfennig, M. Liu, H. J. Snaith, M. B. Johnston, L. M. Herz, *Energy Environ. Sci.* **2014**, *7*, 2269.